

DEPARTMENT OF STATISTICS

University of Wisconsin

1210 West Dayton St.

Madison, WI 53706

TECHNICAL REPORT NO. 1089

January 27, 2004

White Matter Density of Corpus Callosum in Autism:  
2D Voxel-Based Morphometry

<sup>1,2,3</sup>Moo K. Chung, <sup>3</sup>Kim Dalton, <sup>3,4,6</sup>Andrew L. Alexander,  
<sup>3,5,6</sup>Richard J. Davidson

<sup>1</sup>Department of Statistics

<sup>2</sup>Department of Biostatistics and Medical Informatics

<sup>3</sup>Keck Laboratory for Functional Brain Imaging and Behavior

<sup>4</sup>Department of Medical Physics

<sup>5</sup>Department of Psychology, <sup>6</sup>Department of Psychiatry

University of Wisconsin-Madison

Madison, WI 53706

# White Matter Density of Corpus Callosum in Autism: 2D Voxel-Based Morphometry

<sup>1,2,3</sup>Moo K. Chung\*, <sup>3</sup>Kim Dalton, <sup>3,4,6</sup>Andrew L. Alexander,  
<sup>3,5,6</sup>Richard J. Davidson

<sup>1</sup>Department of Statistics

<sup>2</sup>Department of Biostatistics and Medical Informatics

<sup>3</sup>Keck Laboratory for Functional Brain Imaging and Behavior

<sup>4</sup>Department of Medical Physics

<sup>5</sup>Department of Psychology, <sup>6</sup>Department of Psychiatry

University of Wisconsin-Madison

Madison, WI 53706

January 27, 2004

## Abstract

Autism is a neurodevelopmental disorder affecting behavioral and social cognition but there is little understanding about the link between the functional deficit and its underlying neuroanatomy. We applied a 2D version of voxel-based morphometry in differentiating the white matter concentration of the corpus callosum for the group of 16 high functioning autistic and 12 normal subjects. Using the white matter density as an index for neural connectivity, autism is shown to exhibit less white matter concentration in the region of the splenium removing the effect of age based on the general linear model framework. Further it is shown that the smaller corpus callosum size in autism is due to hypoplasia rather than atrophy.

---

\*Corresponding Author. Email: [mchung@stat.wisc.edu](mailto:mchung@stat.wisc.edu) Web page: <http://www.stat.wisc.edu/~mchung>

# 1 Introduction

Autism is a neurodevelopmental disorder of brain function that has begun to attract *in vivo* structural magnetic resonance imaging (MRI) studies in the region of the corpus callosum (Piven *et al.*, 1996, 1997; Egaas *et al.* 1995, Hardan *et al.*, 2000; Manes *et al.*, 1999). There is little understanding about the link between the functional deficit and the underlying abnormal anatomy in autism, which provides motivation for our study. These studies use the Witelson partition or a similar partition scheme of the corpus callosum (Witelson, 1989). Witelson partitioned the mid-sagittal cross-sectional images of the corpus callosum along the maximum anterior-posterior line (Talairach and Tournoux, 1988) and defined the region of the genu, rostrum, midbodies, isthmus and splenium from the anterior to posterior direction. Based on the Witelson partition, there has been a consistent finding in abnormal reduction in anterior, midbody and posterior of the corpus callosum (Brambilla *et al.*, 2003).

Piven *et al.* (1997) compared 35 autistic individuals with 36 normal control subjects controlling for total brain volume, gender and IQ and detected a statistically significant smaller midbody and posterior regions of the corpus callosum in the autistic group. Manes *et al.* (1999) compared 27 low functioning autistic individuals with 17 normal controls adjusting for the total brain volume. They found a smaller corpus callosum compared to the control group in genu, rostrum, anterior midbody, posterior midbody and isthmus but did not find statistically significant differences in the rostrum and the splenium although the sample mean of the rostrum and splenium size are smaller than that of the control group. Hardan *et al.* (2000) compared 22 high functioning autistic to 22 individually matched control subjects and showed smaller genu and rostrum of the corpus callosum adjusting for the total brain volume based on the Witelson partition. The smaller corpus callosum size was considered as an indication of a decrease in interhemispheric connectivity. They did not detect other regions of significant size difference. For an extensive review of structural MRI studies for autism that have been published between 1966 and 2003, one may refer to Brambilla *et al.* (2003).

The shortcoming of the Witelson partition is the artificial partitioning. The Witelson partition may dilute the power of detection if the anatomical difference occurs near the partition boundary. Alternative voxel-wise approaches that avoid predefined regions of interests (ROI) have begun to be used in structural autism studies. Vidal *et al.* (2003) used the tensor-based morphometry (TBM) to show reduced callosal thickness in the genu, midbody and splenium in autistic children. Abell *et al.* (1999) used voxel-based morphometry (VBM) (Wright *et al.*, 1995; Ashburner and

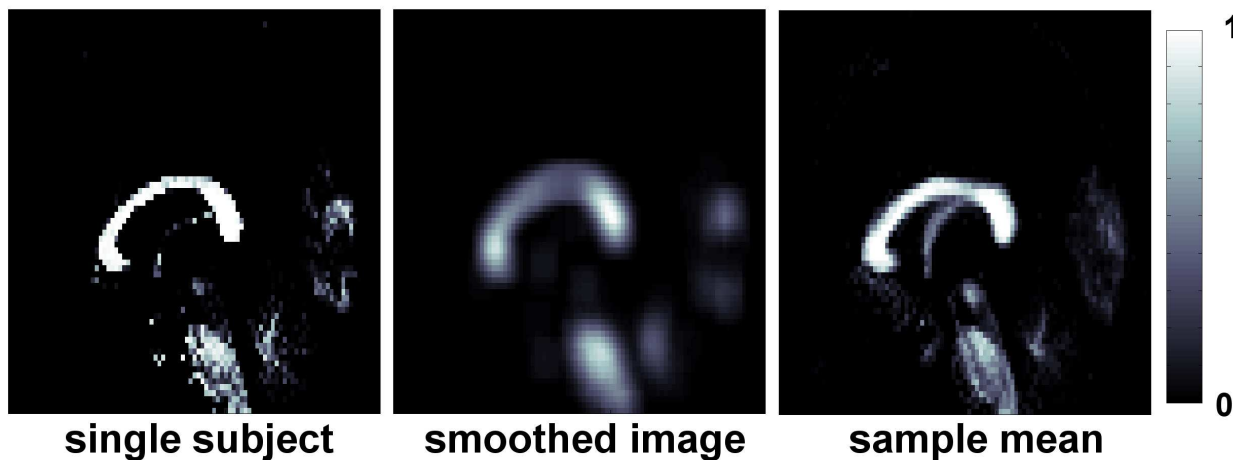


Figure 1: Left: white matter segmentation of an individual midsagittal MRI from SPM'99. Middle: 2D Gaussian kernel smoothing of the white matter segmentation with 12mm FWHM. Right: the sample mean of the smoothed white matter density for control groups.

Friston, 2000, 2001; Good *et al.*, 2001) in high functioning autism to show decreased gray matter volume in the right paracingulate sulcus, the left occipito-temporal cortex and increased amygdala and periamygdaloid cortex. The advantage of the VBM framework over the Witelson partition approach is that it is completely automated and does not require artificial partitioning of the corpus callosum that introduces undesirable bias. Further it is not restricted to *a priori* ROIs enabling us to perform the statistical analysis at each voxel level and to pinpoint the exact location of the anatomical differences. Let us review the basis of VBM and its connection to ROI morphometry.

## 2 Methods

### Voxel-based morphometry

VBM as implemented in SPM'99 computer package (Wellcome Department of Cognitive Neurology, London, UK, <http://www.fil.ion.ucl.ac.uk/spm>) starts with normalizing each structural MRI to the standard SPM template and segmenting it into white and gray matter and cerebrospinal fluid based on a Gaussian mixture model (Ashburner and Friston, 1997, 2000). Based on a prior probability of each voxel being the specific tissue type, a Bayesian approach is used to get a better estimate of the posterior probability. This Bayesian update of the probability is iterated many times until the probability converges. This probability is usually referred to as *density*. Note that

this is not physical density so it should be interpreted probabilistically. There has been on going discussions on the amount of image registration and modulation by the determinant of the Jacobian of deformation fields in VBM (Bookstein, 2001; Ashburner and Friston, 2001; Mehta *et al.*, 2003).

In our study, we applied the 2D version of VBM on the midsagittal cross section of 3D MRI (Figure 1). Let  $p(x), x \in \mathbb{R}^2$  be the white matter density of the 2D midsagittal cross section of corpus callosum  $\Omega$ . Denote  $\mathbf{1}_\Omega(x) = 1$  if  $x \in \Omega$  and 0 otherwise. The shape of  $\Omega$  is random and we associate it with probability  $p(x)$ ,

$$P(x \in \Omega) = p(x).$$

Then the area of the corpus callosum  $\Omega$  is given by

$$A(\Omega) = \int \mathbf{1}_\Omega(x) dx.$$

From this, by taking the expectation, we estimate the area of corpus callosum as

$$\hat{A}(\Omega) = \mathbb{E}A(\Omega) = \int \mathbb{E}\mathbf{1}_\Omega(x) dx = \int p(x) dx. \quad (1)$$

So the sum of the white matter density over all voxels gives an approximation to the area of the corpus callosum. In this context, ROI morphometry used in Piven *et al.* (1997), Hardan *et al.* (2000) and Manes *et al.* (1999) can be viewed as a subset of VBM framework. For instance ROI morphometry based on Witelson partition can be performed by segmenting the normalized 2D midsagittal images.

The white matter density is a probability ranging between 0 and 1 so it is not exactly normally distributed. To make it more normal, one may apply the *logit* transform

$$p \rightarrow \frac{1}{2} \ln \frac{p}{1-p}.$$

However we did not perform the logit transform since we adapted the usual Gaussian kernel smoothing with relatively large 12mm FWHM to make the white matter density more normal (Figure 1). For detailed distributional assumptions, one may refer to Ashburner and Friston (2000) and Salmond *et al.* (2002). Let  $K_\sigma$  be a Gaussian kernel that follows bivariate normal  $N(0, \sigma^2 I)$ . Kernel smoothing of scalar function  $p$  is defined as convolution

$$\int K_\sigma * p(x) dx = \int \int K_\sigma(x-y)p(y) dy dx = \int p(y) dy. \quad (2)$$

From equation (1) and (2) it can be seen that the area estimate

$$\hat{A}(\Omega) = \int K_\sigma * p(x) dx$$

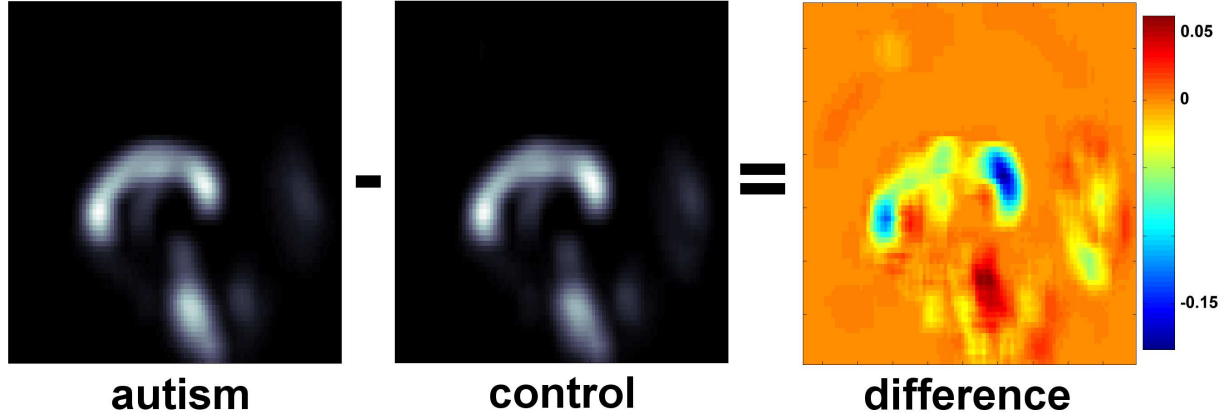


Figure 2: The sample mean of the white matter density of the autistic group (left) and the control group (middle) respectively. The third figure is the difference of the sample mean. We are interested in testing if this difference is statistically significant. Simply comparing the white matter density difference, the autistic group shows less white matter concentration in the genu and the splenium of the corpus callosum.

is invariant under scale  $\sigma$  change. This can be used to estimate the corpus callosum area from VBM white matter density maps. Assuming normality for kernel smoothing  $K_\sigma * p$ ,  $\hat{A}(\Omega)$  would be normal so the usual statistical tests based on normality can be applicable.

## Two sample $t$ -test

Let  $p_a^1, \dots, p_a^m (m = 16)$  be the white matter density for autism and  $p_c^1, \dots, p_c^n (n = 12)$  be the white matter density for controls at a given voxel. We assume  $p_a^i \sim N(\mu_a, \sigma_a^2)$  and  $p_c^j \sim N(\mu_c, \sigma_c^2)$  independently. We denote the sample mean and the variance of  $p_a^i$  and  $p_c^j$  by  $\bar{p}_a, \bar{p}_c, S_a^2, S_c^2$  respectively.

First we test if the autistic group has more white matter variability in the corpus callosum:

$$H_0 : \sigma_a^2 = \sigma_c^2 \text{ vs. } H_1 : \sigma_a^2 \geq \sigma_c^2.$$

Under the null assumption, the ratio of the sample variances  $S_a^2/S_c^2$  has an  $F$  distribution with  $m - 1$  and  $n - 1$  degrees of freedom. The  $F$ -map is given in Figure 3 where the splenium of the autistic group shows statistically significant larger variability. In this region, the autism shows nine times more variability ( $p$ -value of 0.0004). Now we test if the white matter density difference between the autistic group and the control group is statistically significant (Figure 2):

$$H_0 : \mu_a = \mu_c \text{ vs. } H_1 : \mu_a \leq \mu_c, \quad (3)$$

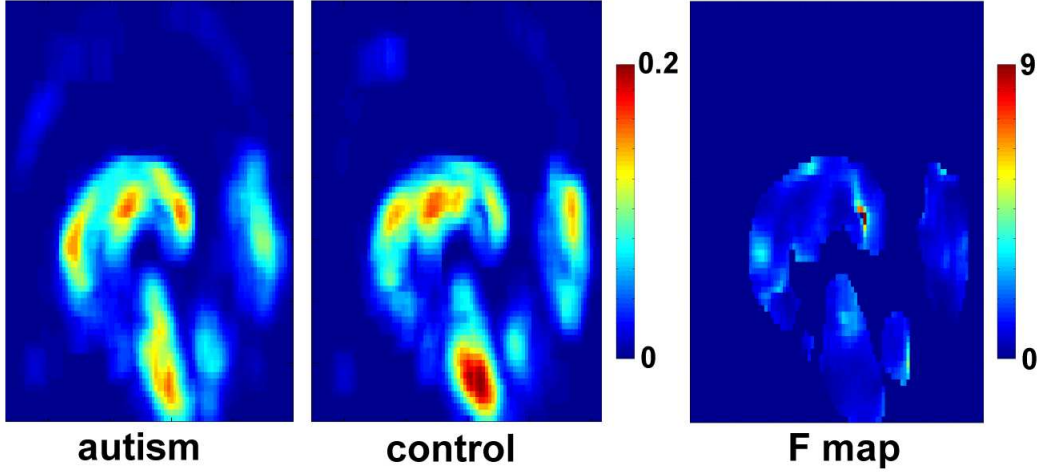


Figure 3: The sample standard deviations of autism (left) and control (middle) respectively. The last figure shows the  $F$ -map showing upto 9 times more variability of the white matter concentration in the splenium of the autistic group. The genu and the midbody also show larger white matter concentration variability but they are not as predominant as the splenium.

The classical test statistic  $T$  for the Behrens-Fisher problem depends on the unknown nuisance parameter  $\sigma_a$  and  $\sigma_c$  that are estimated by sample variances (Tsui and Weerahandi, 1989):

$$T = \frac{\bar{d}_a - \bar{d}_c}{\sqrt{S_a^2/m + S_c^2/n}} \sim t_{d.f.}$$

where the degrees of freedom  $d.f.$  of the  $t$ -distribution is estimated by

$$d.f. = \frac{(S_a^2/m + S_c^2/n)^2}{(S_a^2/m)^2/(m-1) + (S_c^2/n)^2/(n-1)}.$$

However, since the degrees of freedom  $d.f. = m + n - 2 = 26$  is relatively high in our study, we may pool the variance and use the pooled two sample  $t$ -statistic

$$T = \frac{\bar{d}_a - \bar{d}_c}{S_p \sqrt{1/m + 1/n}} \sim t_{m+n-2},$$

where the pooled variance  $S_p^2 = ((m-1)S_a^2 + (n-1)S_c^2)/(m+n-2)$ . In fact we did not see much difference between  $t$ -statistic images in two cases so we will pool the variances for the two sample  $t$ -test. The advantage of pooling the variance is that the statistical distribution becomes exact. However care should have taken when pooling the variance since it can be shown to lead to erroneous conclusions when it is applied when population variance are different for small sample size. An alternate approach would be to use the concept of *generalized p-value* which provides exact probability statments in the presence of unisance parameters (Tsui and Weerahandi, 1989).

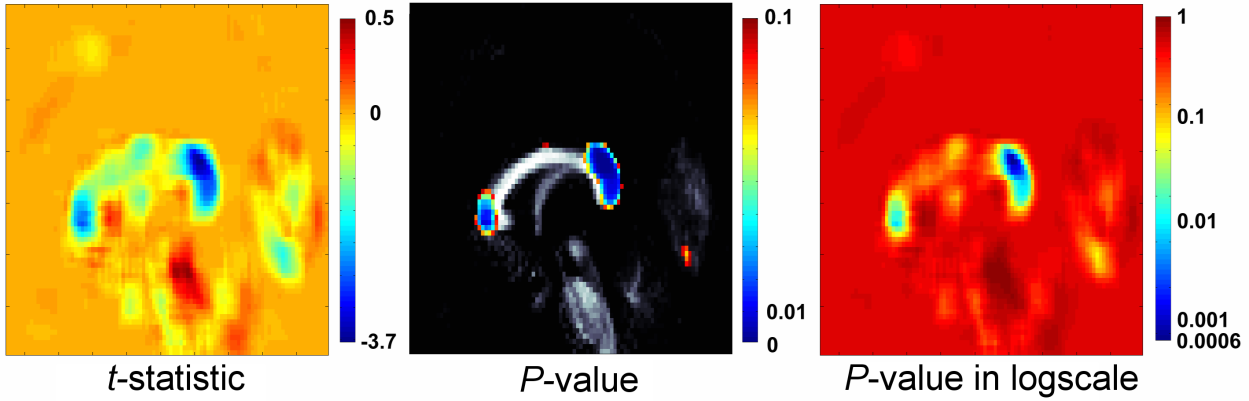


Figure 4: Left: two sample  $t$  statistics. Middle:  $p$ -value map thresholded at 0.1. Right:  $p$ -value represented in logarithmic scale. The log scale is useful in displaying  $p$ -value map. The splenium and the genu of the corpus callosum show huge white matter deficiency in autism compared to control.

In the place of a test statistic, they use so called generalized test variable and the corresponding  $p$ -value can be computed exactly. For multiple comparison that account for spatially correlated errors, one may use the result of the random field theory (Worsley *et al.*, 1996), the false positive rates approach (Genevese *et al.*, 2002; Benjamini and Hochberg, 1995) or random permutation tests (Nichols and Holmes, 2002) but we will not discuss it in this paper.

## General linear models

Since all subjects are different in age and IQ, there might be confounding effects of age and IQ on the white matter density. Previous anatomical studies in the corpus callosum suggest this (Brambilla *et al.*, 2003). On the other hand, deformation-based morphometry and tensor-based morphometry in the normal developmental studies in children show that there is relative brain tissue growth in the corpus callosum over time (Chung *et al.*, 2001; Thompson *et al.*, 2000). In particular, Chung *et al.* (2001) showed white matter local volume increase in the midbody, isthmus and splenium of the corpus callosum in 28 normal subjects from 12 to 16 years (Figure 5). In our study, the age for the control group is  $17.1 \pm 2.8$  and for the autism group it is  $16.1 \pm 4.5$  years. The age ranges for two groups are somewhat compatible; however, there might be still age effect on the white matter difference. To evaluate any possible effect of age on the white matter density, we first fit linear models

$$\text{density} = \lambda_1 + \lambda_2 \cdot \text{age} \quad (4)$$

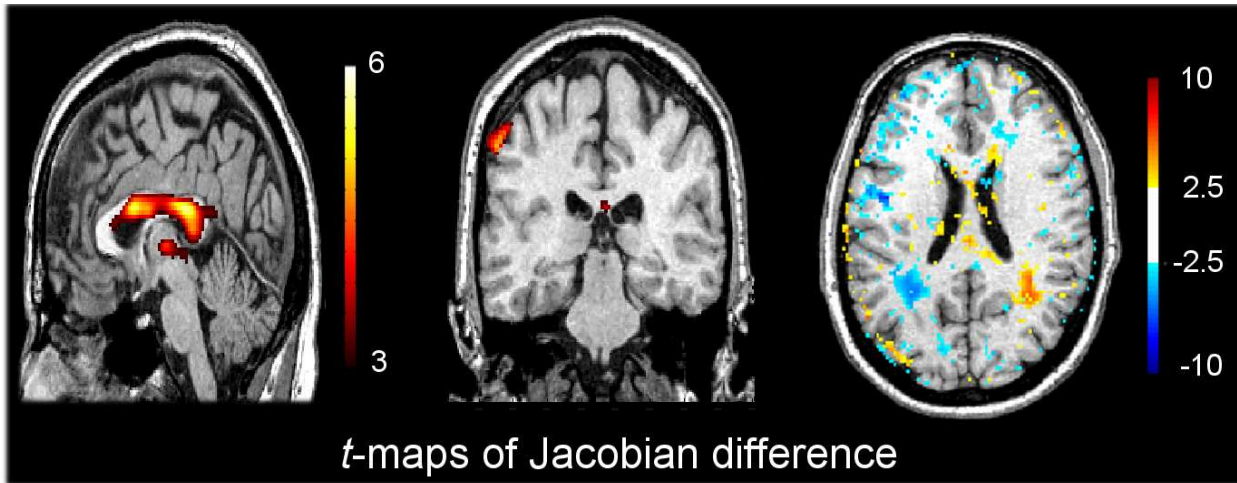


Figure 5: The  $t$  statistic maps of brain volume change for children. The Jacobian of the deformation fields is computed and used as a metric for measuring local volume in Chung *et al.* (2001). Red color indicates the brain tissue growth over time and blue color is atrophy. The midbody, isthmus and splenium show white matter volume increase.

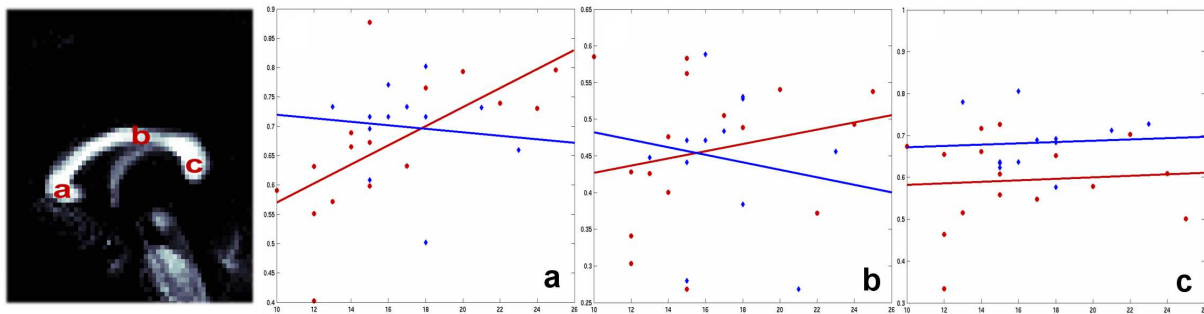


Figure 6: The simple linear fit correlating the white matter density to age at the genu (a), midbody (b) and the splenium (c). Red color is the autism group and blue color is the control group. The splenium seems to show obvious white matter deficiency in autism but group differences in the genu and the midbody are unclear due to different associations with age in each group.

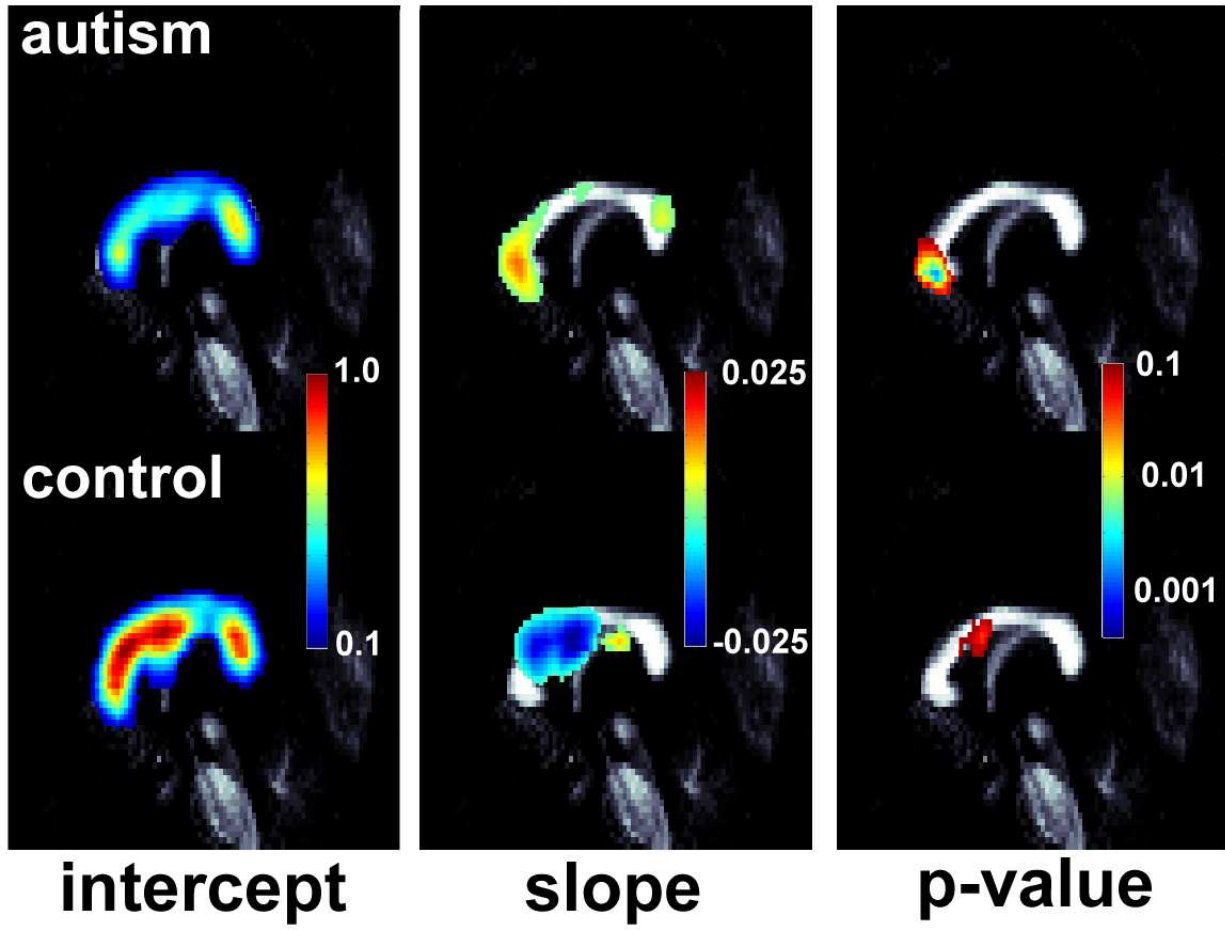


Figure 7: Linear regression of the white matter density on age. Linear growth model density =  $\lambda_1 + \lambda_2 \cdot \text{age}$  is fitted for each group separately.  $\lambda_1$  is the intercept and  $\lambda_2$  is the slope of the regression line. The autistic group shows lower white matter density compared to the control at lower age but gains white matter over time while the control group shows decreasing white matter density with age. The control group shows 2.5%/year decrease in white matter concentration in the midbody while the autistic group shows 2.5%/year increase of white matter in the genu. *F*-test was performed for the fit of the linear model and its *P*-value is computed.

to each group separately using the least-squares method at each voxel (Figure 6 and Figure 7). The linear model fit shows the dynamic pattern of different white matter density changes over time between groups. The pattern of growth in the corpus callosum seems different. The autistic group shows lower white matter density compared to the control group at the lower age but gains white matter over time while the control group shows decreasing white matter density with age. There thus appears to be age differences for at least some regions of the corpus callosum and these should be accounted for.

One approach for removing the age effect would be to modulate the white matter density such that the age effect will not be present. First we estimate  $\lambda_1$  and  $\lambda_2$  for each group via the least squares method. Then adjust the white matter density  $d(t)$  at time  $t$  via transform

$$d(t) \rightarrow d(t) + \hat{\lambda}_2(\bar{t} - t),$$

where  $\hat{\lambda}_2$  is the least-squares estimation of  $\lambda_2$  and  $\bar{t}$  is the mean age of both the controls and autistic combined together. This has an effect of modulating the densities measured at different age to fixed reference age  $\bar{t}$ . A more general approach would be to use a general linear model (GLM). The general linear model (GLM) is a flexible framework that can be used in localizing the region of white matter concentration that are related to covariates such as age, IQ, gender and handedness. Statistical frameworks such as the analysis of variance (ANOVA), the multivariate analysis of variance (MANOVA), the analysis of covariance (ANCOVA) and the multivariate analysis of covariance (MANCOVA) can be viewed as special cases of the GLM.

We consider the following GLM:

$$\text{density} = \lambda_1 + \lambda_2 \cdot \text{age} + \beta_1 \cdot \text{group} + \epsilon,$$

where the dummy variable group is 1 for autism and 0 for control. In this formulation, we do not have separate linear equations as before but combine autism and control group data together and have a single linear equation. A similar linear model formulation in the VBM is used in localizing the region of the gray matter maturation in children (Paus *et al.*, 1999). To formulate the problem in somewhat general fashion, let  $\mathbf{z} = (z_1, \dots, z_k)$  to be nuisance variables such as age and IQ and  $\mathbf{x} = (x_1, \dots, x_p)$  to be the variable of interest such as group. Then we have GLM in the following form

$$p = \mathbf{z}\lambda + \mathbf{x}\beta + \epsilon$$

where  $\lambda = (\lambda_1, \dots, \lambda_k)'$  and  $\beta = (\beta_1, \dots, \beta_p)'$ . We assume the usual mean zero Gaussian noise.

Then we test

$$H_0 : \mathbb{E}p = \mathbf{z}\lambda \text{ vs. } H_1 : \mathbb{E}p = \mathbf{z}\lambda + \mathbf{x}\beta. \quad (5)$$

It is equivalent to testing

$$H_0 : \beta = 0 \text{ vs. } H_1 : \beta \neq 0.$$

The fit of model is measured by the residual sum of squares or the sum of the squared errors (SSE):

$$\begin{aligned} \text{SSE}_0 &= \sum_{i=1}^{m+n} (p_i - \mathbf{z}_i \hat{\lambda}_0)^2, \\ \text{SSE}_1 &= \sum_{i=1}^{m+n} (p_i - \mathbf{z}_i \hat{\lambda}_1 - \mathbf{x}_i \hat{\beta}_1)^2, \end{aligned}$$

where  $\hat{\lambda}_0, \hat{\lambda}_1, \hat{\beta}_1$  are the least squares estimators of the parameters and  $\mathbf{z}_i$  and  $\mathbf{x}_i$  are data for  $i$ -th subject. Under  $H_0$ ,

$$F = \frac{(\text{SSE}_0 - \text{SSE}_1)/p}{\text{SSE}_0/(m+n-p-k)} \sim F_{p, m+n-p-k}. \quad (6)$$

The larger the  $F$  value, it is more unlikely to accept  $H_0$ . For our data, we are testing for group difference controlling for age effect so  $k = 2$  and  $p = 1$ .

## Subjects and image acquisition

Gender and handedness affect the corpus callosum anatomy (Witelson, 1985; Witelson, 1989; Luders, 2003) so all the 16 autistic and 12 control subjects used in this study are right-handed males except one subject who is ambidextrous. Sixteen autistic subjects were recruited for this study from a list of individuals with a diagnosis of high functioning autism in the Madison and Milwaukee area maintained for research purposes by the Waisman center at the University of Wisconsin-Madison. Diagnoses were confirmed with the Autism Diagnostic Interview - Revised (ADI-R) or clinical interview administered by a trained and certified psychologist at the Waisman center. All participants met DSM-IV criteria for autism or Asperger's pervasive developmental disorder. Twelve healthy, typically developing males with no current or past psychological diagnoses served as a control group. The average age for control is  $17.1 \pm 2.8$  and autism is  $16.1 \pm 4.5$  which is in compatible age range.

$T_1$ -weighted MRI scans were obtained with a 3 Tesla GE scanner (flip angle  $30^\circ$ , field of view 24cm,  $256 \times 192$  matrix size with 1.2mm slice thickness). MRIs were normalized and segmented

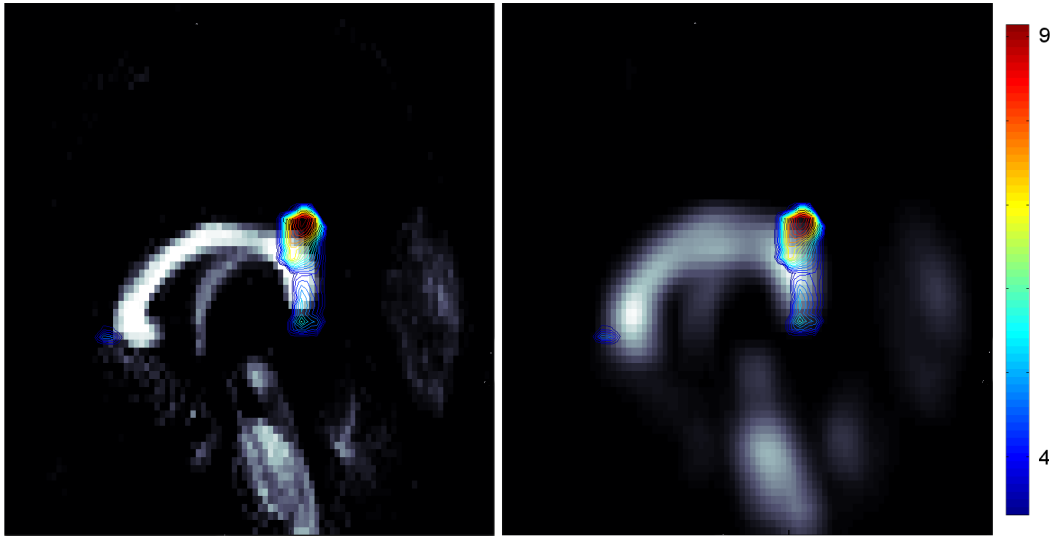
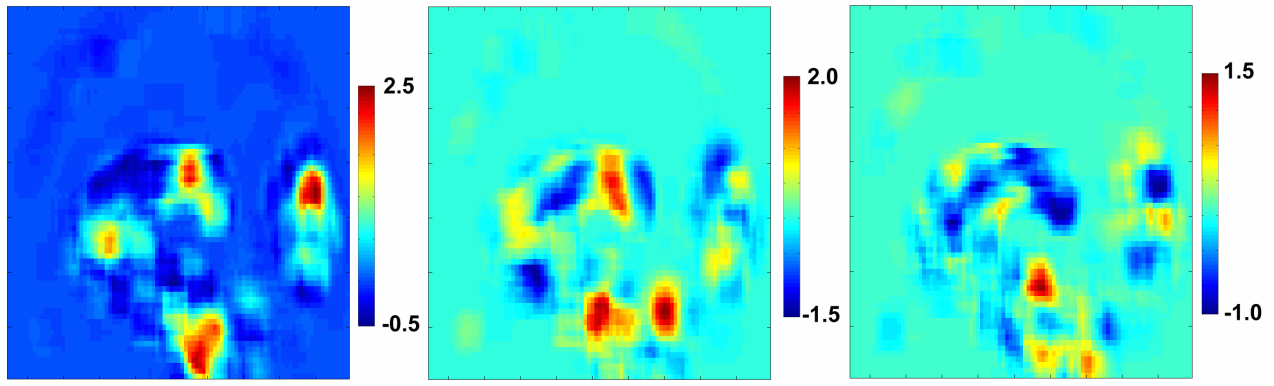


Figure 8: Contour plots of  $F$ -map showing the statistically significant white matter density difference controlling for age effect superimposed on top of the normalized mean of 12 control subjects. Left:  $F$ -map is superimpose on top of the sample mean of the normalized images. Right:  $F$ -map is superimposed on top of the sample mean of the normalized and smoothed images. It shows white matter density difference occurs in the genu and the splenium.

as described in the previous section. Then the midsagittal cross sections of the white matter segmented images showing the corpus callosum were extracted and smoothed with 12mm 2D Gaussian kernel (Figure 1).

### 3 Results

First we fit the white matter density change over age via linear growth model (4). The white matter increase of 2.5% per year in the genu of the autistic group and decrease of 2.5% per year in the midbody of the control group are statistically significant (Figure 6 and 7). Since there is no age effect in the splenium, the white matter difference in that region should be largely due to the group difference while the white matter difference detected in the genu may be in fact due to a possible age effect. So we refitted GLMs (5) as described in the previous section and computed  $F$  statistic map. We found statistically significant white matter deficiency in the genu ( $P$ -value = 0.044) and the splenium ( $P$ -value = 0.005, maximum  $F$ -value = 9.5). It is interesting to note that the splenium is the region of high variability for the autistic group (Figure 3). In the splenium we found 9 times more variable white matter density ( $p$ -value of 0.0004).



**t statistics of random permutations**

Figure 9: Null data is constructed by randomly selecting 8 from 16 autism and 6 from 12 controls and combine them together to form a group consisting of 14 subjects. Combining the remaining 14 subjects formed the second group. Then two sample  $t$  tests are performed on these null data. For 3 different random permutations, the statistical significance of white matter difference is much lower than the real data indicating no image processing artifacts.

Comparing GLM results (Figure 8) with the two sample  $t$ -test results not taking account for the age effect (Figure 4), we see similar a  $P$ -value map in both cases indicating the age effect in our study is negligible due to the compatible age range between groups.

To check for possible image processing artifacts, we applied our statistical tests on null data constructed from randomly selecting 8 from 16 autism and 6 from 12 controls and combining them together to form a new group consisting of 14 subjects. Combining the remaining 14 subjects formed the second new group. Afterwards, the same statistical tests were performed on the null data revealing no significant result other than due to randomness. For instance the two sample  $t$ -test is performed in null data and the resulting  $t$ -map shows insignificant results for three random permutations (Figure 9). A similar approach of generating null data and checking possible image processing artifacts has been proposed in Chung *et al.* (2003) for a child brain development study.

## 4 Discussion

The 2D version of the voxel-based morphometry was used in the midsagittal cross section of MRI quantifying the white matter deficiency in high functioning autism. Accounting for an age effect, statistically significant white matter deficiency in the genu and splenium of the corpus callosum was detected in the autistic group but there is no significant difference in the midbody. This may

suggest impaired inter-hemispheric connectivity in frontal and particularly temporal and occipital regions. It is interesting to note that Piven *et al.* (1996) found increased volume of the parietal, temporal and posterior lobes but not the frontal lobes in autism compared to normal control. The deficit in splenium white matter may be associated with the abnormalities in face processing and particularly in the identification of emotion in faces (Dalton et al., 2003). In normal subjects, faces activate the right fusiform area and the verbal identification of the emotion in a face likely requires transfer of information between the hemispheres in the splenium region. The deficit found here in the autism group may at least in part underlie the abnormalities in emotional face processing observed in this group (Dalton et al., 2003).

Linear growth models were fitted for autism and control groups separately to show different pattern of white matter density change over time. Subjects with autism shows lower white matter concentration at the lower age range in almost all part of the corpus callosum but the white matter density increases over age. On the other hand, the normal control group shows a higher concentration of the white matter at younger ages, but decreasing density particularly in the midbody with increase in age. The smaller callosal size in the genu and splenium might be attributed to hypoplasia rather than atrophy. In particular we found a statistically significant 2.5%/year increase of the white matter in the genu for the autistic group.

A similar result was obtained using tensor-based morphometry where Vidal *et al.* (2003) compared 15 autistic subjects of age  $9.9 \pm 3.2$  years to a group of 13 control subjects of age  $10 \pm 2.1$  years. They found the most significant reduction of the corpus callosum size in the genu, splenium and midbody in decreasing order. The difference with our voxel-based morphometry result might be due to the different morphometric techniques plus manual segmentation used in Vidal *et al.* (2003) while no manual segmentation of any sort was applied in our study.

## Acknowledgements

Authors wish to thank Terry Oacks and Andrew Fox of the Keck brain imaging laboratory for valuable discussions on VBM, Kam Sui of the department of the statistics for the discussion on the generalized  $p$ -value, John Ashburner for pointing out the image orientation convention in SPM'99 package. This work was funded by Wisconsin Alumni Research Foundational (WARF), NIMH U54 MH066398 and by a NARSAD Distinguished Investigator Award to RJD.

## References

1. Abell, F., Krams, M., Ashburner, J., Passingham, R., Friston, K., Frackowiak, R., Happé, F., Frith, C., Frith, U. 1999. The neuroanatomy of autism: a voxel-based whole brain analysis of structural scans. *NeuroReport* **10**:1647-1651.
2. Ashburner, J., Friston, K.J. 2001. Why Voxel-based morphometry should be used. *NeuroImage* **14**:1238-1243.
3. Ashburner, J., Friston, K.J. 2000. Voxel-based morphometry-the method, *NeuroImage*. **11**:805-821.
4. Ashburner, J., Friston, K.J. 1997. Multimodal image coregistration and partitioning - a unified framework, *NeuroImage* **6**:209-217.
5. Benjamini, Y and Hochberg, Y. 1995. Controlling the false discovery rate: a practical and powerful approach to multiple testing. *J. Roy Stat Soc, Ser B.* **57**:289-300.
6. Bookstein, F.L. 2001. Voxel-based morphometry should not be used with imperfectly registered images. *NeuroImage* **14**:1454-1462.
7. Brambilla, P., Hardan, A., di Nemi, S. U., Perez, J., Soares, J.C., Barale, F. 2003. Brain anatomy and development in autism: review of structural MRI studies, *Brain Research Bulletin*, **61**:557-569.
8. Brambilla, P., Nicoletti, M.A., Sassi, R.B., Mallinger, A.G., Frank, E., Kupfer, D.J., Keshavan, M.S., Soares, J.C. 2003. Magnetic resonance imaging study of corpus callosum abnormalities in patients with bipolar disorder, *Biol. Psychiatry* **54**:1294-1297.
9. Chung, M.K., Worsley, K.J., Robbins, S., Paus, P., Taylor, J., Giedd, J.N., Rapoport, J.L., Evans, A.C. 2003. Deformation-based surface morphometry with an application to gray matter deformation, *NeuroImage* **18**:198-213.
10. Chung, M.K., Worsley, K.J. , Paus, T., Cherif, C., Giedd, J.N., Rapoport, J.L and Evans, A.C. 2001. A unified statistical approach to deformation-based morphometry, *NeuroImage* **14**:595-606.
11. Dalton, K.M., Anderle, M., Fisher, R., Schaeffer, H., Alexander, A.L. and Davidson, R.J. 2003. Brain function in individuals diagnosed with autism during discrimination of emotion.

The proceeding of the 9th Annual Meeting of the Organization for Human Brain Mapping, New York, NY.

12. Egaas, B., Courchesne, E., Saitoh, O. 1995. Reduced size of the corpus callosum in autism. *Arch. Neurol.* **52**:794-801.
13. Genovese, C.R., Lazar, N.A., Nichols, T.E. 2002. Thresholding of statistical maps in functional neuroimaging using the false discovery rate. *NeuroImage* **15**:870-878.
14. Good, C.D., Johnsrude, I., Ashburner, J., Henson, R.N.A., Friston, K.J., Frackowiak, R.S.J., 2001. A voxel-based morphometric study of ageing in 465 normal adult human brains. *Neuroimage* **14**:21-36.
15. Hardan, A.Y., Minshew, N.J., Keshavan, M.S. 2000. Corpus callosum size in autism. *Neurology* **55**:1033-1036.
16. Good, C.D., Johnsrude, I.S., Ashburner, J., Henson, R.N.A., Friston, K.J., and Frackowiak, R.S.J. 2001. A Voxel-Based Morphometric Study of Ageing in 465 Normal Adult Human Brains, *NeuroImage*. **14**:21-36.
17. Luders, E., Rex, D.E., Narr, K.L., Woods, R.P., Janke, L., Thompson, P.M., Mazziotta, J.C., Toga, A.W. 2003. Relationships between sulcal asymmetries and corpus callosum size: gender and handedness effects. *Cerebral Cortex* **13**:1084-1093.
18. Manes, F., Piven, J., Vrancic, V., Plebst, C., Starkstein, S.E. 1999. An MRI study of the corpus callosum and cerebellum in mentally retarded autistic individuals, *J. Neuropsychiatry Clin Neurosci.*, **11**:470-474.
19. Mehta, S., Grabowski, T.J., Trivedi, Y. and Damasio, H. 2003. Evaluation of voxel-based morphometry for focal lesion detection in individuals, *NeuroImage* **20**:1438-1454.
20. Nichols, T.E. and Holmes, A.P. 2002. Nonparametric permutation tests for functional neuroimaging experiments: a primer with examples. *Human Brain Mapping* **15**:1-25.
21. Paus, T., Zijdenbos, A., Worsley, K., Collins, D. L., blumenthal, J, Giedd, J.N., Rapoport, J.L., Evans, A.C. 1999. Structural maturation of neural pathways in children and adolescents: in vivo study. *Science* **283**:1908-1911.

22. Pettey, D.J., Gee, J.C., Sexual dimorphism in the corpus callosum: a characterization of local size variations and a classification driven approach to morphometry. *NeuroImage*. **17**:1504-1511.
23. Piven, J., Bailey, J., Randon, B.J., Arndt, S., An MRI study of the corpus callosum in autism. 1997. *Am. J. Psychiatry* **154**:1051-1056.
24. Piven, J., Bailey, A.S., Andreasen, N. 1996. Regional brain enlargement in autism: a magnetic resonance imaging study. *J. Am. Acad. Child Adolesc. Psychiatry* **35**: 530-536.
25. Salmond, C.H., Ashburner, J., Vargha-Khadem, F., Connelly, A., Gadian, D.G. and Friston, K.J. 2002. Distributional assumptions in voxel-based morphometry. *NeuroImage* **17**:1027-1030.
26. Talairach, J. and Tournoux, P. 1988. *Co-planar Stereotaxic Atlas of the Human Brain: 3-Dimensional Proportional System - an Approach to Cerebral Imaging*, Thieme Medical Publishers, New York, NY.
27. Thompson, P. M., Giedd, J. N., Woods, R. P., MacDonald, D., Evans, A. C., and Toga, A. W. 2000. Growth patterns in the developing human brain detected using continuum-mechanical tensor mapping. *Nature* **404**: 190193.
28. Vidal, C.N., DeVito, T.J., Hayashi, K.M., Drost, D.J., Williamson, P.C., Craven-Thuss, B., Herman, D., Sui, Y., Toga, A.W., Nicolson, R. and Thompson, P.M. 2003. Detection and visualization of corpus callosum deficits in autistic children using novel anatomical mapping algorithms, Proc. International Society for Magnetic Resonance in Medicine (ISMRM) 2003, Toronto, Canada.
29. Witelson, S.F. 1985. The brain connection: the corpus callosum is larger in left-handers. *Science* **229**:665-668.
30. Witelson, S.F. 1989. Hand and sex differences in the isthmus and genu of the human corpus callosum. *Brain*. **112**:799-835.
31. Wright, I.C., McGuire, P.K., Poline, J.-B., Travers, J.M., Murray, R.M., Frith, C.D., Frackowiak, R.S.J., and Friston, K.J. 1995. A voxel-based method for the statistical analysis of gray and white matter density applied to schizophrenia. *NeuroImage* **2**:244-252.